


Blood Flow Deficits and Cerebrovascular Changes in a Dietary Model of Hyperhomocysteinemia

ASN Neuro
Volume 11: 1–13
© The Author(s) 2019
Article reuse guidelines:
sagepub.com/journals-permissions
DOI: 10.1177/1759091419865788
journals.sagepub.com/home/asn



David J. Braun¹ , Erin Abner^{1,2}, Vikas Bakshi¹,
Danielle S. Goulding³, Elizabeth M. Grau¹, Ai-Ling Lin^{1,4},
Christopher M. Norris^{1,4}, Tiffany L. Sudduth¹, Scott J. Webster¹,
Donna M. Wilcock^{1,5}, and Linda J. Van Eldik^{1,6,7}

Abstract

Elevated homocysteine in the blood, or hyperhomocysteinemia, is a recognized risk factor for multiple causes of dementia including Alzheimer's disease. While reduction of homocysteine levels can generally be accomplished in a straightforward manner, the evidence regarding the cognitive benefits of this approach is less clear. To identify adjunct therapeutic targets that might more effectively restore cognition, the present series of experiments characterizes early and later cerebrovascular changes in a model of hyperhomocysteinemia. Sex-balanced groups of adult C57BL/6J mice were administered a diet deficient in vitamins B₆, B₁₂, and B₉ (folate) and supplemented with excess methionine. They were subsequently assessed for changes in cerebral blood flow, memory, blood–brain barrier permeability, and selected vascular-associated genes. Blood flow deficits and barrier permeability changes occurred alongside changes in memory and in genes associated with metabolism, endothelial nitric oxide signaling, barrier integrity, and extracellular matrix remodeling. Significant sexually dimorphic responses to the diet were also detected. Taken together, these data deepen our understanding of a major contributor to dementia burden.

Keywords

blood–brain barrier, cerebral blood flow, cerebrovascular disease, dementia, vascular biology

Received May 9, 2019; Received revised June 20, 2019; Accepted for publication June 21, 2019

Introduction

Elevated blood levels of the amino acid homocysteine, termed hyperhomocysteinemia (HHcy), is a risk factor for cognitive impairment and dementia (Smith et al., 2018). Strikingly, the population attributable risk of Alzheimer's disease (AD) due to HHcy is estimated to be as high as 31% (Van Dam & Van Gool, 2009; Smith et al., 2018), and it follows that successful treatment of this condition may significantly reduce AD incidence. This is especially important given the high prevalence of HHcy in elderly persons (Janson et al., 2002; Salles-Montaudon et al., 2003) combined with the projected growth of AD in coming decades (Alzheimer's Association, 2018). Improved understanding of how HHcy affects cognition may therefore be crucial to reducing future dementia burden.

¹Sanders-Brown Center on Aging, University of Kentucky, Lexington KY, USA

²Department of Epidemiology, University of Kentucky, Lexington KY, USA

³Kentucky Neuroscience Institute, University of Kentucky, Lexington KY, USA

⁴Department of Pharmacology & Nutritional Sciences, University of Kentucky, Lexington KY, USA

⁵Department of Physiology, University of Kentucky, Lexington KY, USA

⁶Department of Neuroscience, University of Kentucky, Lexington KY, USA

⁷Spinal Cord and Brain Injury Research Center, University of Kentucky, Lexington KY, USA

Vikas Bakshi is now at Charles River Laboratory, Wilmington, MA, USA.

Scott J. Webster is now at Virtuoso Surgical, Inc., Nashville, TN, USA.

Corresponding Author:

Linda J. Van Eldik, University of Kentucky College of Medicine, 101 Sanders-Brown Bldg., 800 S. Limestone Street, Lexington KY 40536, USA.

Email: linda.vaneldik@uky.edu



Homocysteine is a nonpeptide amino acid produced from methionine, the levels of which are kept low by enzymes that depend on vitamins B₆, B₁₂, and B₉ (folate) for their function (Selhub, 1999). Accordingly, deficits in one or more of these is commonly associated with increased homocysteine levels in patients (Novaković et al., 2018), and data from several meta-analyses of randomized controlled trials demonstrate the efficacy of B vitamin supplementation on lowering homocysteine levels (Durga et al., 2007; Smith et al., 2010; Ford & Almeida, 2012; Clarke et al., 2014). While encouraging in that such interventions are safe, inexpensive, and effective, these same meta-analyses also provide mixed evidence as to whether this reduction translates to improved cognitive outcomes (Price et al., 2018). While reduction of homocysteine levels is an important goal, it is likely that concomitant amelioration of homocysteine-associated damage is necessary to provide maximal benefit. For example, disruption of the methylation cycle is well characterized in this condition (Selhub, 1999; Fuso et al., 2008), and supplementation with substances to reduce this disruption (e.g., betaine, S-adenosyl methionine) shows benefit in rodent models without reduction in plasma homocysteine levels (Fuso et al., 2012; Chai et al., 2013). Aside from disruptions to the methylation cycle, vascular injury is also a well-characterized aspect of HHcy and highly relevant to cognitive function (Hainsworth et al., 2016). Much of this information comes from peripheral vasculature or *in vitro* systems, however, and therefore may not be representative of changes occurring in the specialized cerebrovasculature.

The present series of experiments therefore aims to characterize early- and later-stage changes in cerebrovascular function resulting from chronic dietary-induced HHcy. HHcy was induced for variable times in sex-balanced groups of male and female C57BL/6J mice beginning at 12 weeks of age. This was achieved with a diet deficient in folate, vitamin B₆, and vitamin B₁₂ and supplemented with methionine as previously published (Sudduth et al., 2013, 2017). Longitudinal changes in cerebral blood flow (CBF) and corresponding cognitive deficits were assayed, along with cross-sectional changes in plasma homocysteine, blood–brain barrier (BBB) permeability, and vascular-associated genes. Our results show early and progressive deficits in CBF and BBB integrity, corresponding with alterations in genes associated with extracellular matrix remodeling, barrier function, energy metabolism, and nitric oxide signaling. Although not specifically designed to detect them, the experiments also revealed significant sexually dimorphic responses.

Methods

Animals and Experimental Diet

Male and female C57BL/6J mice were purchased from The Jackson Laboratory (strain #664) and aged to 12 weeks before placement on experimental diets. All chow was procured from Envigo (Huntingdon, United Kingdom). Mice were randomized into groups, housed 1 to 5 animals per cage (503.22 usable cm²), and maintained in a room at 23°C ± 2°C with a 14/10 hr light/dark cycle beginning at 6:00 a.m. They were maintained on standard rodent chow (Envigo Teklad #2918) prior to administration of custom diets, also purchased from Envigo. The HHcy diet (TD.97345) lacks folate, vitamin B₆, and vitamin B₁₂ and is supplemented with excess methionine (7.7 g/kg). The control diet (TD.01636) is nutritionally matched but with lower methionine (3.0 g/kg) and normal levels of vitamins B₆, B₁₂, and folate (see Supplements 1 and 2 for further details). Sulfathiazole was not administered to inhibit B vitamin synthesis by the gut microbiota. Diets were refreshed on a weekly basis, at which time animals and remaining food were weighed. Food consumption was estimated as an average per mouse per day within each cage. Mice had ad libitum access to water and chow. Environmental enrichment included a 5 × 5 cm cotton Nestlet™ (Ancare, Bellmore, NY, USA), paper shredding, a Backless Shack mouse house (Shepherd Specialty Papers, Watertown, TN, USA), and 1/2 × 1/2 × 2" aspen chew sticks (Lomir Biomedical Inc, Quebec, Canada).

The data were collected across two separate studies. In the first, mice were randomized into 2 sex-balanced groups to receive 12 weeks of HHcy ($n = 18$, 9 M and 9 F) or control diet ($n = 10$, 5 M and 5 F) and undergo longitudinal neuroimaging followed by spatial memory testing in the radial arm water maze (RAWM). In the second, sex-balanced groups of 12 mice (6 M and 6 F) were randomized into 6 groups to receive HHcy or control diet for 4, 8, or 12 weeks prior to sacrifice and tissue collection. Sample sizes were determined based upon previously published studies of cognitive deficits in this model (Chai et al., 2013). All animal experiments were performed in compliance with the principles of animal care and experimentation in the Guide for the Care and Use of Laboratory Animals and approved by the Institutional Animal Care and Use Committee of the University of Kentucky. Mice that reached greater than 20% weight loss prior to the conclusion of the study were humanely euthanized and excluded from behavioral analyses. All sections of this report adhere to the ARRIVE guidelines for reporting animal research (Kilkenny et al., 2010). In total, 11 out of 30 mice assigned to HHcy diet for 12 weeks (6 in the first study, 5 in the second) reached

the 20% weight loss criterion and were euthanized between 10 and 12 weeks. Where data from these mice are included in pathological analyses, the figures refer to a 10- to 12-week rather than 12-week time point. Notably, only female mice reached humane end point criteria.

Measurement of CBF by Pseudocontinuous Arterial Spin Labeling

After 6 and 10 weeks on experimental diet, mice from the first study underwent magnetic resonance imaging (MRI) scans to determine CBF by pseudocontinuous arterial spin labeling (pCASL) as previously reported (Ma et al., 2018). Experiments were performed using a 7 Tesla magnet (ClinScan, Bruker BioSpin, Germany) at the Magnetic Resonance Imaging and Spectroscopy Center at the University of Kentucky. Mice were anesthetized with 4.0% isoflurane and maintained during imaging in a 1.2% isoflurane and air mixture using a nose cone. Heart rate (90–110 bpm), respiration rate (50–80 breaths/min), and rectal temperature ($37 \pm 1^\circ\text{C}$) were continuously monitored and maintained. A whole-body volume coil and mouse brain surface coil were used for transmission and receiving, respectively. T2-weighted structural images were acquired with field of view = $18 \times 18 \text{ mm}^2$, matrix = 256×256 ; slice thickness = 1 mm, 10 slices, repetition time = 1,500 ms, and echo time = 35 ms. Paired control and labeled images were acquired in an interleaved manner, with a train of Hanning window-shaped radiofrequency pulses. Duration/spacing = 200 μs , 25 degree flip angle, slice-selective gradient = 9mT/m, and labeling duration = 2,100 ms. Two-dimensional multislice spin-echo planar imaging was used with field of view = $18 \times 18 \text{ mm}^2$, matrix = 128×128 , slice thickness = 1 mm, 10 slices, repetition time = 4,000 ms per segment, echo time = 35 ms, and 120 repetitions. Image analysis was performed with codes written in-house with MATLAB (MathWorks, Natick, MA, USA) to obtain quantitative CBF in ml/g per minute in the hippocampus (Alsop et al., 2015).

RAWM Test of Spatial Learning and Memory

Testing in the RAWM occurred at about 12 weeks on HHcy diet, to allow for recovery from the neuroimaging end points. RAWM was run according to the protocols previously described (Alamed et al., 2006; Webster et al., 2015). Briefly, the maze consisted of six arms in a circular tank filled with water containing nontoxic white tempera paint. The tank was enclosed by black curtains arranged in a square, with geometric extramaze visual cues affixed to three of four curtain sides. A circular platform was placed at the end of one of the arms, approximately 1 to 2 cm below the water's surface to provide an escape. Animals were split into two groups and tested in a

back-to-back 3-day paradigm. Each day consisted of 15 trials (45 trials total), with the first 12 trials on Day 1 alternating between hidden and visible (flagged) platform. The platform was hidden for all trials after the first 12. Trials were run in two blocks of six trials and one block of three trials on the first day, and three blocks of five trials on Days 2 and 3. Mice were run in groups of six at a time, alternating by block to provide time to rest. Mice alternated between all possible start arms throughout the study, with the goal arm held constant for all animals. Errors were defined as an entry of the entire body of the mouse (excluding tail) into the nongoal arms. Errors and swim speed were tracked via overhead camera and Noldus EthoVision XT (Noldus, Leesburg, VA, USA).

Nesting Assay

The nesting assay was performed as previously described (Deacon, 2006; Webster et al., 2015) with mice from the second study. The day prior to sacrifice, mice were singly housed in a new cage with fresh bedding and a new Nestlet. Paper shredding, Shephard Shacks, and chew sticks were removed. Mice were left in the normal housing room overnight (14–16 hr). Subsequently, two observers blinded to the experimental conditions scored the quality of the nests according to a semiquantitative 5-point scale: (1)—Nestlet not noticeably touched, >90% intact; (2)—Nestlet partially torn up, 50% to 90% remaining intact; (3)—shredded >50% but without identifiable nesting site and bedding spread around cage; (4)—identifiable but flat nest, >90% of the Nestlet torn up with the material gathered within one quarter of the cage floor area; (5)—a near perfect nest where >90% of the Nestlet is torn up and the nest is crater shaped with walls higher than mouse body for at least half of the circumference. Scores were assigned in half-point increments from 1 to 5 and averaged between the observers.

Brain Tissue Collection and Plasma Homocysteine Measurement

Subsequent to behavioral assays, all mice were anesthetized with 5% isoflurane, transcardially perfused with 1X ice-cold phosphate-buffered saline (PBS - Corning, Manassas, VA, USA, #46-013-CM) for 5 min at 10 ml/min and rapidly decapitated for brain extraction. Prior to perfusion, arterial blood was collected from the left ventricle of mice while anesthetized and placed into EDTA tubes (Greiner Bio-One North America, Monroe NC, USA, #454428) for separation of plasma by centrifugation ($2000 \times g$ for 20 min at room temperature). Plasma supernatant was removed, flash-frozen in liquid nitrogen, and stored at -80°C . Samples were diluted 1:5–1:10 in ARCHITECT Multi-Assay Manual Diluent and

delivered to the University of Kentucky Clinical Laboratory for homocysteine measurement on an ARCHITECT i2000SR analyzer (Abbott Laboratories, Chicago, IL, USA).

Tissue for biochemistry was taken from the left hemisphere, which was dissected and immediately flash-frozen in liquid nitrogen and stored at -80°C . The entire right hemisphere was processed for immunohistochemistry: postfixed in 4% paraformaldehyde (Millipore Sigma, Burlington, MA, USA, #441244) at 4°C overnight and cryoprotected in 30% sucrose (MP Biomedicals, Solon, OH, USA, #902978) at 4°C for 48 hr. The first ~ 4 mm of the anterior pole of the hemisphere was removed, and a Leica Biosystems (Wetzlar, Germany) SM 2010R sliding microtome with freezing stage was used to cut 30- μm coronal sections posteriorly until the level of the cerebellum. Sections were stored in cryoprotectant (50% 1X PBS, 25% ethylene glycol, 25% glycerol) at -20°C , and staining procedures were carried out on free-floating sections using every 10th section.

BBB Permeability Measurement by Immunoglobulin G Immunohistochemistry

For immunoglobulin G (IgG) detection, samples underwent endogenous peroxidase quench for 30 min (0.3% hydrogen peroxide in methanol) followed by incubation for 1 hr at 4°C with a 1:250 concentration of biotinylated anti-mouse IgG antibody (Jackson ImmunoResearch, West Grove, PA, USA, #115-065-205) in PBS with 0.2% TX-100. Subsequently, tissue was incubated for 1 hr in ABC solution (Vector Laboratories, Burlingame, CA, USA, #PK-4000) and developed with 3,3'-diaminobenzidine tetrahydrochloride hydrate (Millipore Sigma #D5637). PBS was used for all washes. Slides were imaged at $20\times$ using an Aperio ScanScope XT digital slide scanner (Leica Biosystems), and cortex was outlined using the Aperio ImageScope software (Leica Biosystems) as previously reported (Webster et al., 2015). The Aperio positive pixel count algorithm was used to quantify the amount of staining in the region, with background threshold adjusted to tissue from control animals. Blinded personnel performed the quantification.

Quantitative Reverse-Transcriptase Polymerase Chain Reaction

RNA was isolated from a piece of frontal cortex using the RNeasy Plus Mini Kit (Qiagen, Germantown, MD, USA, #74136) according to manufacturer's instructions. Briefly, cortical tissue was weighed and homogenized in an appropriate volume of buffer, and genomic DNA removed with the gDNA eliminator column. The samples were mixed with ethanol and RNA bound to the RNeasy column, washed, and eluted in RNase-free water.

Quantity of RNA and 260/280 absorbance ratios were assessed using a NanoDrop spectrophotometer (ThermoFisher Scientific, Waltham, MA, USA). Reverse transcription was performed with the High-Capacity cDNA Reverse Transcription kit (Applied Biosystems, Foster City, CA, USA, #4368814) according to manufacturer's protocol. Real-time polymerase chain reaction was performed on a ViiA 7 Real-Time PCR System (Applied Biosystems) using custom TaqMan[®] Array Cards (ThermoFisher Scientific, #4342253) with TaqMan Fast Advanced Master Mix (ThermoFisher Scientific, #4444557). See Table 1 for a complete list of genes and probes included on the array. The probes for *Col4a3* and *Angpt13* had one nondetect each. Probes with more than one nondetect were excluded from analysis: *Mmp10*, *Plg*, *Sele*, and *Selp*. Relative gene expression was calculated using the $2^{-\Delta\Delta\text{CT}}$ method and log₂ normalized. Hypoxanthine-guanine phosphoribosyltransferase (HPRT) and 18S ribosomal RNA (18S) were included as housekeeping genes, with values for genes of interest normalized to the geometric mean of the two. A total of 42 genes were analyzed.

Images and Statistical Analyses

Analyses were performed in JMP Pro 14 (SAS Institute Inc, Cary, NC, USA) or GraphPad Prism 7 (GraphPad

Table 1. TaqMan Custom Gene Array.

Gene symbol	Assay ID	Gene symbol	Assay ID
18S	Hs99999901_s1	Itgb3	Mm00443980_ml
Abcb1a	Mm00440761_ml	Lef1	Mm00550265_ml
Adamts1	Mm00477355_ml	Mmp10	Mm01168399_ml
Aggf1	Mm00546486_ml	Mmp2	Mm00439498_ml
Amot	Mm00462731_ml	Mmp9	Mm00442991_ml
Angpt1	Mm00456503_ml	Nos3	Mm00435217_ml
Angpt2	Mm00545822_ml	Nostrin	Mm00724960_ml
Angptl1	Mm01291815_ml	Ocln	Mm00500912_ml
Angptl3	Mm00803820_ml	Pdgfb	Mm00440677_ml
Angptl4	Mm00480431_ml	Plg	Mm00447087_ml
Apcdd1	Mm01257559_ml	Sele	Mm00441278_ml
Axin2	Mm00443610_ml	Selp	Mm01295931_ml
Col18a1	Mm00487131_ml	Slc2a1	Mm00441480_ml
Col4a3	Mm00483656_ml	Smo	Mm01162710_ml
Dixdcl1	Mm01175093_ml	Tek	Mm00443243_ml
Fgf1	Mm00438906_ml	Tgfb1	Mm01178820_ml
Fgf2	Mm00433287_ml	Tie1	Mm00441786_ml
Ftl1	Mm00438980_ml	Timp1	Mm00441818_ml
Fzd6	Mm00433387_ml	Timp2	Mm00441825_ml
Hprt	Mm00446968_ml	Tjp1	Mm00493699_ml
Icam1	Mm00516023_ml	Tnfrsf1b	Mm01205928_ml
Itga5	Mm00439797_ml	Tnfrsf19	Mm00443506_ml
Itgav	Mm00434486_ml	Vcam1	Mm01320970_ml
Itgb1	Mm01253230_ml	Vegfa	Mm01281449_ml

Software, La Jolla, CA, USA), with statistical significance level set to $\alpha = .05$. For comparison of two groups, unpaired student's *t* test or nonparametric Mann–Whitney U tests were used. For more than two groups, a one- or two-way analysis of variance (ANOVA) was performed where data met appropriate parametric statistical assumptions, followed by Sidak's post hoc testing. In cases with significant violation of assumptions, the nonparametric Kruskal–Wallis test was used, or data were rank transformed for logistic regression followed by Mann–Whitney U post hoc comparisons (IgG data). Mixed measures ANOVA was used for the RAWM data, with Sidak's post hoc testing where indicated. Figures were created in GraphPad Prism 7. Data are expressed as means with error bars representing standard deviation. Data cited within the text are

reported as $M = \text{mean}$, $SD = \text{standard deviation}$, and $CI = \text{lower 95\% confidence interval, upper 95\% confidence interval}$, except when data are not sufficiently normally distributed. In that case, data are Median, 25th percentile, 75th percentile.

Results

General Health and Observations

Samples from mice in the second study on HHcy diet and a subgroup of mice on control diet ($n = 4$) were analyzed for homocysteine concentration. As expected, mice on HHcy diet achieved elevated homocysteine levels by 4 weeks on diet ($M = 41.04 \mu\text{M}$, $SD = 16.41$, $CI [30.62, 51.47]$; Figure 1(a)). Levels were increased further at 10 to

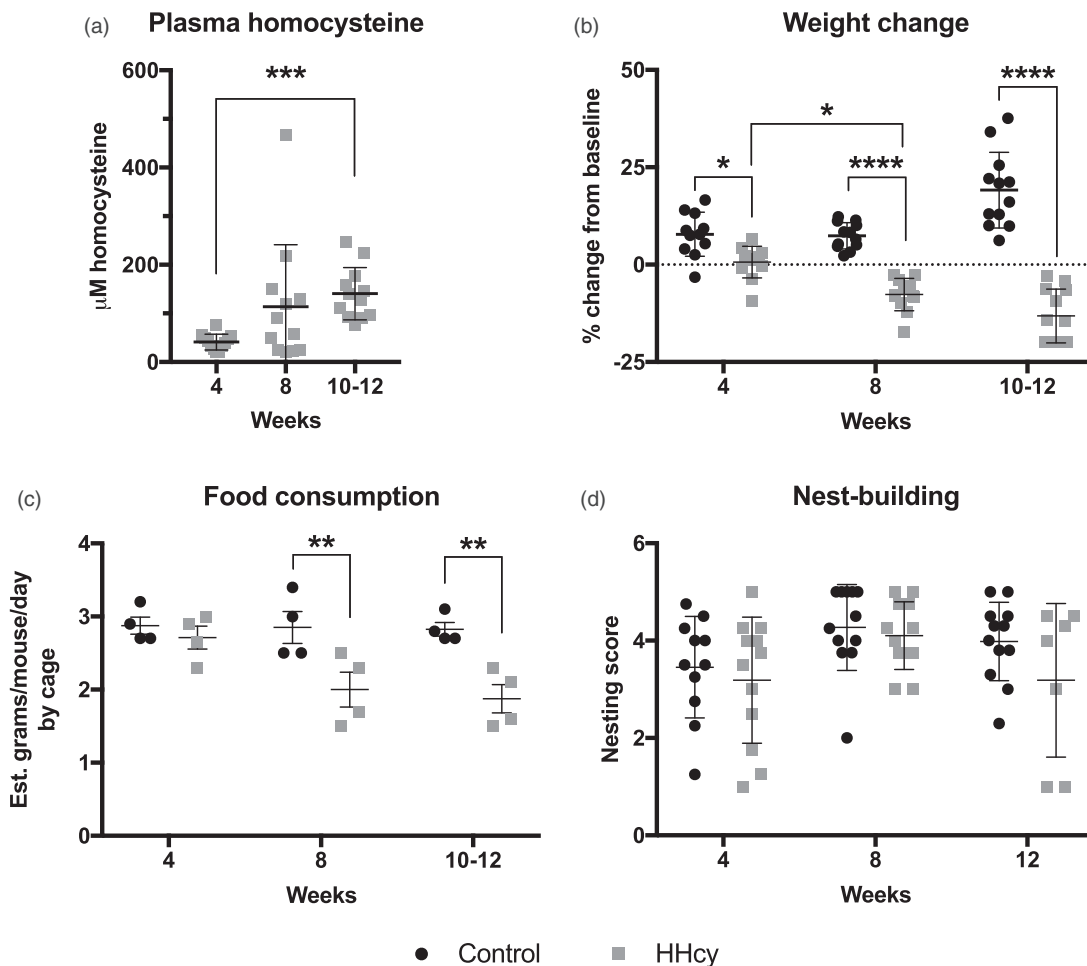


Figure 1. General health and observations. (a) Levels of homocysteine were measured in plasma after 4, 8, and 10 to 12 weeks on HHcy diet. *** $p < .001$ versus 4-week time point, Kruskal–Wallis with Dunn's post hoc testing, $n = 12$ per group. (b) Percent baseline weight change was significantly reduced in HHcy versus control at all time points. This corresponded with a significant reduction in estimated food consumption by 8 weeks as shown in (c), as an average value calculated by cage ($n = 4$ per group). No significant changes in intrinsic nest building were detected after any time on diet (d). $n = 7$ for the 12-week HHcy group and $n = 12$ for all others (see text). * $p < .05$, ** $p < .01$, *** $p < .001$ versus corresponding control group indicated by connector, two-way ANOVA with Sidak's multiple comparison testing, $n = 12$ except where indicated. HHcy = hyperhomocysteinemia.

12 weeks ($M = 140.50 \mu\text{M}$, $SD = 53.57$, $CI [106.50, 174.50]$). All values from mice on control diet were below the $5 \mu\text{M}$ limit of detection, with the exception of one female in the 8-week control group ($7.0 \mu\text{M}$) that had an untreated overgrooming lesion at time of sacrifice (data not shown). In addition to plasma homocysteine increases, mice on HHcy diet for 4 weeks failed to gain weight from baseline ($M = 0.7\%$, $SD = 4.0$, $CI [-1.9, 3.2]$) in contrast to controls ($M = 7.8\%$, $SD = 5.6$, $CI [4.0, 11.6]$; Figure 1(b)). With more time on HHcy diet, mice began losing bodyweight by 8 weeks ($M = -7.7\%$, $SD = 4.1$, $CI [-10.3, -5.2]$), an effect persisting to 10 to 12 weeks ($M = -13.2$, $SD = 6.9$, $CI [-17.6, -8.8]$). Mice on control diet, in contrast, gained weight by the end of the study ($M = 19.1\%$, $SD = 9.7$, $CI [12.9, 25.3]$).

Interestingly, the initial lack of weight gain was not associated with decreased food consumption as mice on control diet average intake ($M = 2.9 \text{ g/day}$, $SD = 0.2$, CI

[2.5, 3.3]) was similar to mice on HHcy diet at 4 weeks ($M = 2.7 \text{ g/day}$, $SD = 0.3$, $CI [2.2, 3.2]$; Figure 1(c)). By 8 weeks, the mice on HHcy diet consumed significantly less ($M = 2.0 \text{ g/day}$, $SD = 0.5$, $CI [1.2, 2.8]$) than controls ($M = 2.9 \text{ g/day}$, $SD = 0.4$, $CI [2.2, 3.50]$). This was similarly true for mice on HHcy diet at 10 to 12 weeks ($M = 1.9 \text{ g/day}$, $SD = 0.4$, $CI [1.3, 2.5]$) versus control ($M = 2.8 \text{ g/day}$, $SD = 0.2$, $CI [2.5, 3.1]$). Despite these observations, no changes in intrinsic nesting behavior were detected due to HHcy at any time (Figure 1(d)). It should be noted, however, that 5 mice in the 12-week group were excluded from the nesting assay due to reaching humane end point criterion.

HHcy Diet Reduces CBF and Causes Deficits in Spatial Learning and Memory

Longitudinal CBF measurements were made using pCASL MRI at both 6 and 10 weeks after diet start.

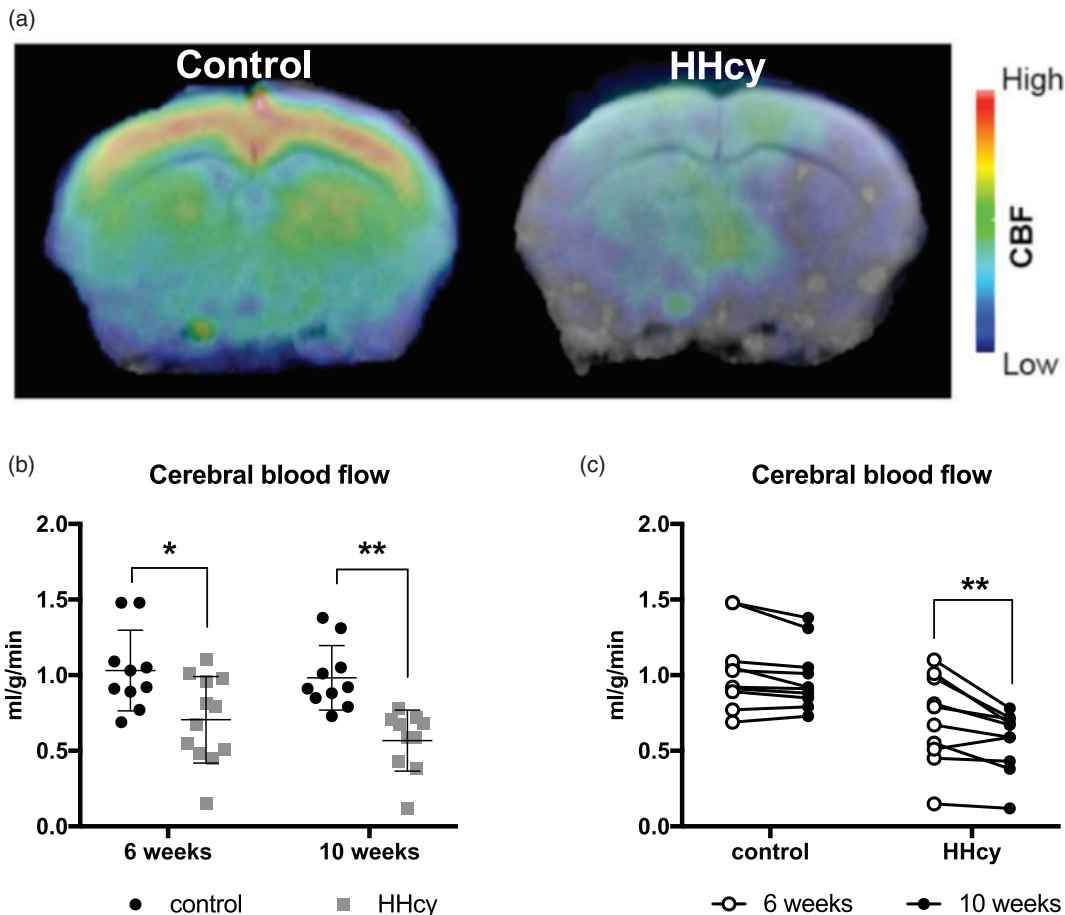


Figure 2. HHcy diet causes early and progressive reductions in cerebral blood flow. Animals underwent pCASL for measurement of CBF after 6 and 10 weeks on HHcy diet. (a) Representative heat map of blood flow data from a coronal section. (b) Mice on HHcy diet had significantly reduced blood flow compared with controls at both 6 and 10 weeks. (c) Within-animal comparisons showed that CBF across time in the HHcy group was significantly reduced with increasing time on diet. Two animals included in the HHcy group in panel (b) were too sick to scan at 10 weeks and excluded from the analysis in panel (c). * $p < .05$, ** $p < .01$ versus corresponding control or group indicated by connecting line, results of two-way ANOVA, $n = 10\text{--}12$ per group. HHcy = hyperhomocysteinemia; CBF = cerebral blood flow.

Figure 2(a) shows a representative heat map of coronal sections. A significant reduction in CBF in the HHcy animals was detected by 6 weeks on diet ($M = 0.71$ ml/g/min, $SD = 0.29$, CI [0.52, 0.89]) relative to controls ($M = 1.03$ ml/g/min, $SD = 0.27$, CI [0.84, 1.2]), and this progressively worsened by 10 weeks ($M = 0.57$ ml/g/min, $SD = 0.20$, CI [0.42, 0.71]; Figure 2(b), (c)). In mice on control diet, CBF after 10 weeks ($M = 0.98$ ml/g/min, $SD = 0.21$, CI [0.83, 1.14]) was not significantly different from that recorded after 6 weeks, as expected.

The reduction in CBF corresponded with significant impairments in spatial learning and memory performance in the RAWM (Figure 3(a), (b)). Number of errors were averaged across blocks of three consecutive trials, and mixed measures ANOVA of the overall learning curves showed a significant time by diet interaction,

$F(14, 280) = 1.96$, $p = .0212$. When errors were averaged by day, mixed measures ANOVA with Sidak's post hoc comparisons found that mice on HHcy diet made significantly more errors during training (Day 1) as well as both testing days (2 and 3). Impairment in long-term memory was also detected as increased errors in the probe trial (the first trial) of each test day (Figure 3(c)). Finally, the average overall velocity was significantly reduced for mice on HHcy diet ($M = 11.70$ cm/s, $SD = 1.16$, CI [10.96, 12.44]) versus control ($M = 14.28$ cm/s, $SD = 1.95$, CI [12.88, 15.68]; Figure 3(d)), indicating a mild swimming impairment. Importantly, the diet effect on total errors remained significant ($p < .0001$) when the average swim speed (centered) was included as a covariate, indicating no evidence that the difference in errors was attributable to the changes in swim speed.

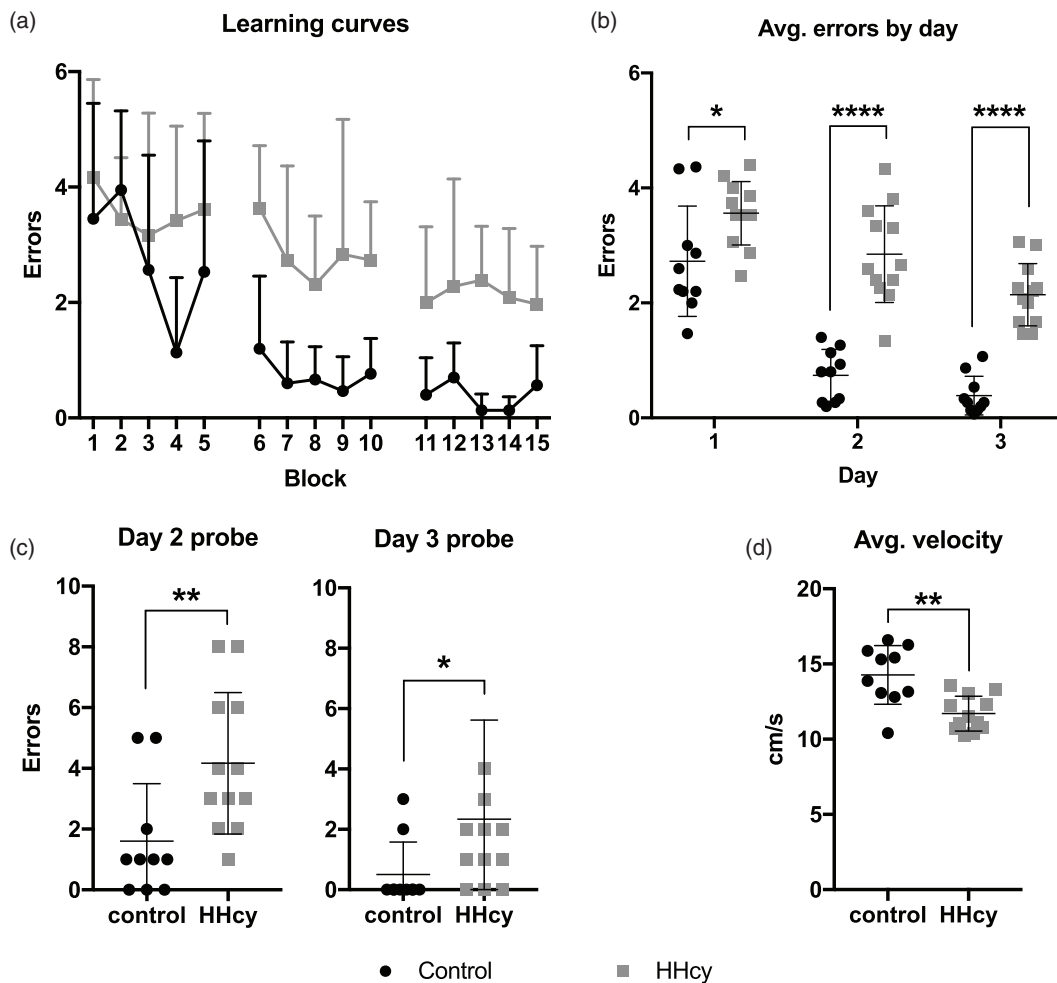


Figure 3. HHcy-associated impairment in spatial learning and memory. (a and b) Mice on HHcy diet made significantly more errors across block and by day than those on control diet. * $p < .05$, **** $p < .001$ versus control, mixed measures ANOVA. (c) HHcy mice also made significantly more errors during the probe trial (first trial of each day) on both testing days * $p < .05$, ** $p < .01$, Mann–Whitney U test. (d) Average velocity across all trials was significantly reduced in the mice on HHcy diet versus controls. ** $p < .01$, student's *t* test. $N = 10$ for control and 12 for HHcy groups. HHcy = hyperhomocysteinemia.

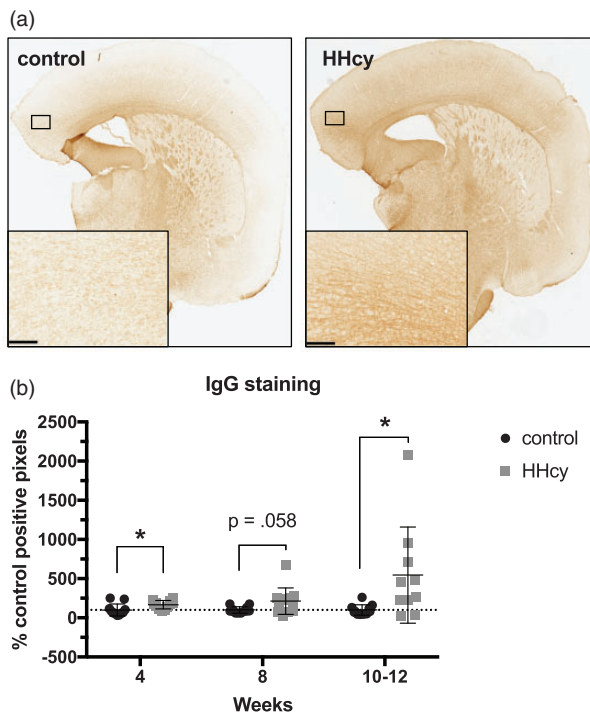


Figure 4. HHcy diet increases blood–brain barrier permeability. Every ~10th section through the cortex for each animal was stained for IgG and positive pixels quantified. (a) Representative section from a mouse on diet for 12 weeks is shown, with inset displaying a higher magnification of the boxed region within cortex. (b) Data are expressed as a percentage of the corresponding controls. IgG staining was significantly elevated versus control at the 4- and 10- to 12-week time points, with a nonsignificant trend toward an increase at 8 weeks. Scale bar = 100 μm . * $p < .05$, ordinal logistic regression of rank-transformed data for overall significance determination, followed by Mann–Whitney U tests between groups at each time point. HHcy = hyperhomocysteinemia; IgG = immunoglobulin G.

HHcy Diet Enhances BBB Permeability and Transcriptional Changes in Vascular-Associated Genes

We have previously reported microhemorrhages in this model after 10 but not 6 weeks on HHcy diet (Sudduth et al., 2017). To quantify earlier and potentially more subtle changes in BBB permeability, we stained for endogenous IgG (Figure 4(a)), which is excluded from the brain parenchyma under nonpathological conditions but not under certain pathological ones (Bowyer et al., 2018). When normalized to control values, levels of IgG staining were significantly increased by 4 ($Mdn = 174.7\%$, 25th percentile = 119.7, 75th percentile = 210.1) and 10 to 12 weeks ($Mdn = 362.4\%$, 25th percentile = 177.9, 75th percentile = 768.4), with a marginally significant trend at 8 weeks ($Mdn = 202.0\%$, 25th percentile = 80.15, 75th percentile = 259.3; Figure 4 (b)). To better characterize underlying pathological changes associated with barrier disruption in this

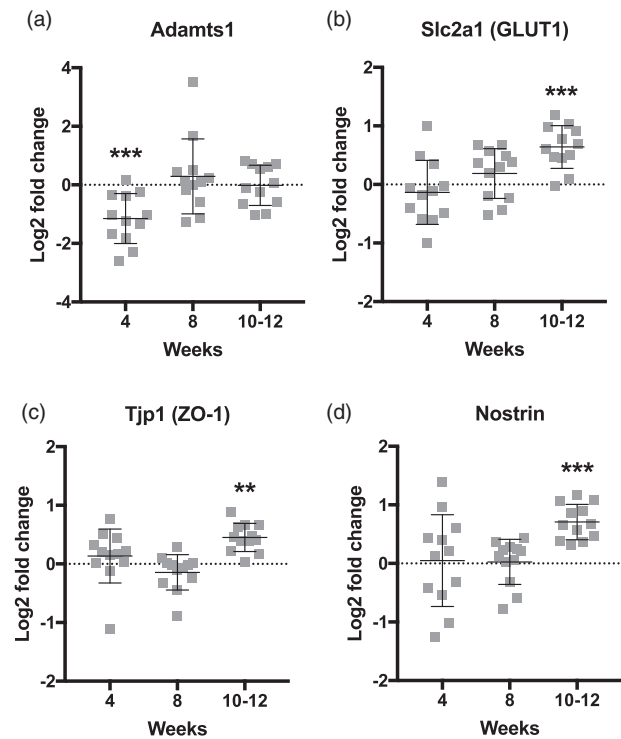


Figure 5. Four vascular-associated genes are significantly altered as a function of time on HHcy diet. Custom TaqMan arrays were run to measure gene expression changes in selected cerebrovascular-associated genes. Data are expressed as log₂ normalized fold changes versus corresponding control group. (a) *Adamts1* is significantly downregulated at 4 weeks on HHcy diet but returns to baseline by 8 weeks. (b to d) *Slc2a1*, *Tjp1*, and *Nostrin* are significantly upregulated by 10 to 12 weeks on HHcy diet. ** $p < .01$, *** $p < .005$ versus corresponding control group, two-way ANOVA, $n = 11$ –12 per group.

model, we measured gene expression levels of 42 preselected vascular-associated genes (Table 1), with log₂ transformation of the fold change values versus control. Of those, four were found to be significantly altered relative to control levels at any time point: *Adamts1*, *Slc2a1* (GLUT-1), *Tjp1* (ZO-1), and *Nostrin* (Figure 5). Interestingly, *Adamts1* was downregulated at 4 weeks ($M = -1.142$, $SD = 0.854$, $CI [-1.694, -0.609]$), with levels normalizing at later time points. In contrast, *Slc2a1* ($M = 0.640$, $SD = 0.364$, $CI [0.408, 0.872]$), *Tjp1* ($M = 0.452$, $SD = 0.239$, $CI [0.300, 0.604]$), and *Nostrin* ($M = 0.708$, $SD = 0.301$, $CI [0.516, 0.899]$) became significantly elevated by 10 to 12 weeks but were unchanged at earlier times.

Given the large effects on BBB permeability, blood flow, and cognition, we were surprised to find differences in only 4 of 42 selected vascular-associated genes. This, combined with the fact that all mice that reached end point criterion were female, led us to consider whether sexually dimorphic responses might be obscuring some of the dietary effects on gene transcription. Further, sex

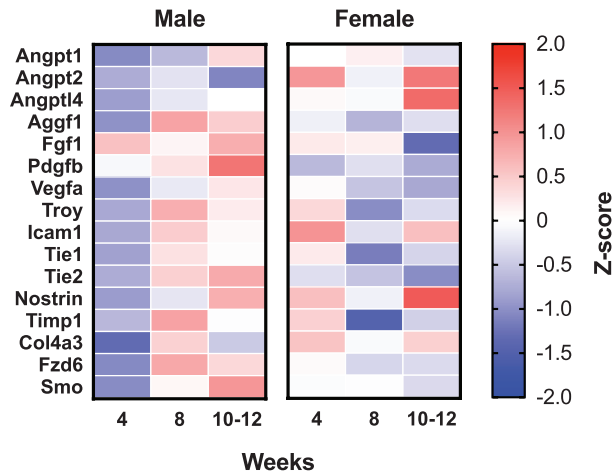


Figure 6. Sixteen genes show sexual dimorphism in response to HHcy diet. Effect of sex on gene expression changes resulting from HHcy diet was examined across all genes on the TaqMan array by two-way ANOVA. Genes with a significant main effect of sex or significant sex by time interaction are included. Log₂ normalized fold change values were converted to standard z scores for comparison.

differences have previously been reported in C57BL/6J mice in response to folate-deficient diet (Ernest et al., 2005). We therefore reexamined where possible the end points with sex as a factor and found that female mice achieved a more rapid elevation of homocysteine levels in addition to increased weight loss in response to the diet (see Supplement 3). We also reanalyzed the gene expression data with sex as a factor and found that 16 genes showed a significant main effect of sex or a significant sex by time interaction when analyzed by two-way ANOVA. Log₂ fold change values for each gene were transformed to z scores and are displayed for comparative purposes in Figure 6. Only 1 of these 16 genes, *Nostrin*, was also significantly changed in the overall group comparison. While interesting, these data must be interpreted with caution due to the fact that the study was not designed at the outset to capture sex differences.

Discussion

HHcy can be subdivided into stages according to blood concentrations, and in mice, these stages have been delineated as mild (12 to 30 μ M), moderate (30 to 100 μ M), and severe (greater than 100 μ M; Ernest et al., 2005). By this standard, all mice in our studies developed moderate HHcy by 4 weeks, 5 of 12 developed severe HHcy by 8 weeks, and 8 of 12 developed severe HHcy by 10 to 12 weeks. This was accompanied by weight loss and a decrease in food consumption, although intrinsic nesting behavior taken as an indicator of general animal health (Gaskill et al., 2013) was not significantly altered at any time point measured. An important caveat here is that 5

of 12 mice in the 12-week group reached humane end point criteria before nesting behavior could be measured, potentially causing an underestimate of diet effects on nesting at that time point. Given that general nutritional deficiencies may contribute to our observations, future studies using less severe methods of HHcy induction (e.g., methionine loading, direct homocysteine supplementation, or genetic models) will be important.

Consistent with previous reports, mice administered HHcy-inducing diet were severely impaired in a spatial memory task by the end of the study (Troen et al., 2008; Sudduth et al., 2013, 2017). We found that this holds true even when alterations in swim speed are taken into account. To our knowledge, this study is the first that has longitudinally assessed CBF changes in response to this type of vitamin-deficient diet. Interestingly, we detected CBF deficits after just 6 weeks, a time before RAWM deficits are manifest in this model (Sudduth et al., 2017); however, future studies should incorporate longitudinal assessment of behavioral changes as well as neuroimaging end points. In addition, future studies would benefit from a more expansive behavioral battery to understand changes across cognitive and noncognitive domains. Nonetheless, these findings are consistent with the notion that hypoperfusion and related changes are likely to be a major upstream contributor to cognitive deficits in this model.

It is unclear whether the impaired CBF is itself due to elevated homocysteine or the vitamin deficiencies in the diet; however, findings from other models of homocysteine elevation indicate that homocysteine itself (or methionine supplementation) is sufficient to disrupt CBF. For example, homocysteine superfusion of rat parietal cortex (Zhang et al., 1998), heterozygous deletion of the cystathionine β synthase gene (Dayal et al., 2004; Kumar et al., 2008), dietary supplementation with homocysteine (Lee et al., 2004), and acutely raised homocysteine resulting from methionine loading (Chao & Lee, 2000) all have negative impacts on various measures of CBF without concomitant vitamin deficiencies.

The chronic deprivation of B vitamins is a well-known cause of anemia in humans (Lanier et al., 2018), and this is true in deficient mice as well (Bills et al., 1992). Indeed, the observed weight loss, loss of appetite, and fatigue/lethargy (indicated by reduced swim speed in the RAWM) are all consistent with an anemic state. Somewhat paradoxically, anemia has been associated with enhanced CBF in both human (Ibaraki et al., 2010) and animal studies (Hudak et al., 1986), and this is generally considered a compensatory mechanism to keep the brain supplied with oxygen. Given that both reduced CBF and putative anemia are simultaneously present in this model, one would expect a chronic hypoxic condition in the brain. Indeed, the hypoxia-responsive gene *Slc2a1* (Patching, 2017) is significantly

upregulated by 10 to 12 weeks. A better characterization of the hypoxic changes under these conditions is worth exploring, as hypoxic damage is a plausible upstream mechanism for a multitude of the pathologies reported in these mice, including those linked to risk for AD such as barrier disruption and neuroinflammation (Daulatzai, 2017). Interestingly, despite the enhanced BBB permeability present in these mice, there was an increase in *Tjp1* mRNA level at 10 to 12 weeks. The discrepancy may be related to changes at the protein level that are not reflected by mRNA, or that trigger compensatory upregulation of the message.

Interestingly, two genes not widely studied in the brain were significantly altered in the overall group comparisons: *Nostrin* and *Adamts1*. *Adamts1* is an extracellular metalloprotease that is known to be expressed in the brain during development (Thai & Iruela-Arispe, 2002) and upregulated after various injuries (Gottschall & Howell, 2015). *Adamts1* also has a role in peripheral inflammatory responses (Rodríguez-Baena et al., 2018) and vascular homeostasis (Oller et al., 2017). Interestingly, one study found that it may also modulate synaptogenesis during development in a sex-specific manner (Howell et al., 2012). The implications of its early reduction in this context are unknown, but it is an intriguing area of future research.

Nostrin is primarily recognized as a mediator of endothelial nitric oxide synthase (eNOS) activity (Michel & Vanhoutte, 2010), and while we did not detect changes in eNOS mRNA levels, there was a significant increase in *Nostrin* by 10 to 12 weeks of HHcy. This is consistent with the known dysfunction of eNOS induced by elevated homocysteine (Yan et al., 2010); in particular, NOSTRIN is known to traffic and sequester eNOS (Zimmermann et al., 2002), and this may represent a previously unknown mechanism through which HHcy disrupts eNOS signaling and contributes to oxidative stress responses in the vasculature (Esse et al., 2019). In addition, NOSTRIN has recently been identified as a major regulator of endothelial cell angiogenic and inflammatory functioning independent of its effects on eNOS (Chakraborty & Ain, 2017). Interestingly, *Nostrin* was the only gene significantly altered by HHcy that also displayed a sexually dimorphic response. In consideration of its pleiotropic nature, this may partially explain some of the other sexually dimorphic responses; however, this remains highly speculative.

Although not originally designed to detect sex differences, our studies demonstrated that female C57BL/6J mice are more sensitive to the HHcy diet than males, at least in terms of weight loss and homocysteine elevation (see Supplement 3). Whether this is due to an increased sensitivity to a specific vitamin deficiency, excess methionine, or a combination of both is unclear. One study found that female C57BL/6J mice have higher

homocysteine levels than males at baseline and after a folate-deficient diet (Ernest et al., 2005). Notably, this is in contrast to humans, where higher estrogen is associated with reduced homocysteine (Morris et al., 2000), and men tend to have higher homocysteine levels at baseline (Sassi et al., 2002). Nonetheless, while men seem more susceptible to the development of elevated homocysteine or vitamin deficiencies (Margalit et al., 2018), they may simultaneously be more resilient to certain deleterious effects of HHcy. For example, some studies find that higher levels of homocysteine correspond with worsened cardiovascular fitness in women but not men (Kuo et al., 2005; Ruiz et al., 2007), although there is some controversy around these findings (Dankner et al., 2009). Whether our observations of sexual dimorphism are inherent to the particular model system chosen or reflective of relevant human biology are important areas for future investigation.

As mentioned in the Introduction section, disrupted DNA methylation is an important aspect of this model, both as a direct result of the dietary intervention (Jiang et al., 2007; Fuso et al., 2008, 2012) and likely contributed to by hypoperfusion (Wu et al., 2013). Follow-up studies into the methylation status of those genes found to be differentially expressed in the brain, as well as genome-wide alterations in methylation, are therefore warranted. In addition, controlled manipulation of homocysteine levels could help parse which mechanisms are more or less involved at different clinically relevant levels of homocysteine elevation. For example, milder chronic elevations might have a detrimental effect primarily mediated through epigenetic mechanisms, while severe elevations might contribute more to the well-described oxidative or inflammatory changes. Any treatment aiming to undo the damage may therefore have to target an array of pathological disruption, which might vary depending on the severity of HHcy.

Finally, the mice used for these experiments were young adults and therefore less reflective of the demographics of the older patient population that tends to have elevated homocysteine and B vitamin deficiencies and are at risk for dementia. Subsequent studies in older mice therefore may provide further crucial insight into how these factors interact with aging. Similarly, a study design incorporating a recovery period from the HHcy diet with assessment of potential persistent pathology will help to elucidate therapeutic targets that might, in combination with interventions designed to lower homocysteine levels, reduce overall dementia burden.

Acknowledgments

The authors would like to acknowledge Edgardo Dimayuga for technical assistance and Drs. Josh Morganti and Adam Bachstetter for scientific advice.

Author Contributions

D. J. B. wrote the article and analyzed the data. V. B. and A. L. measured and analyzed CBF. S. J. W. performed the RAWM testing. E. M. G. stained and outlined brain sections for IgG. D. J. B. isolated RNA and ran quantitative PCR. D. J. B. and D. S. G. performed nesting assays and harvested tissue. D. S. G., T. L. S., and D. J. B. administered diet and monitored the mice throughout the studies. E. A. assisted with statistical analyses. L. J. V. E., A. L., C. M. N., D. M. W., and D. J. B. conceived of and planned the experiments. All authors contributed to editing the article and approved the final draft.

Declaration of Conflicting Interests

The author(s) declared no potential conflicts of interest with respect to the research, authorship, and/or publication of this article.

Funding

The author(s) disclosed receipt of the following financial support for the research, authorship, and/or publication of this article: This work was supported by National Institutes of Health grants R01NS093920, R01AG054459, K01AG040164, F32AG058456, and a Postdoctoral Fellowship from the Weston Brain Institute.

ORCID iD

David J. Braun  <https://orcid.org/0000-0002-6967-0489>

Supplemental Material

Supplemental material for this article is available online.

References

- Alamed, J., Wilcock, D. M., Diamond, D. M., Gordon, M. N., Morgan, D. (2006). Two-day radial-arm water maze learning and memory task; robust resolution of amyloid-related memory deficits in transgenic mice. *Nat Protoc*, *1*, 1671–1679.
- Alsop, D. C., Detre, J. A., Golay, X., Günther, M., Hendrikse, J., Hernandez-Garcia, L., Lu, H., MacIntosh, B. J., Parkes, L., Smits, M., van Osch, M. J., Wang, D. J., Wong, E. C., Zaharchuk, G. (2015). Recommended implementation of arterial spin-labeled perfusion MRI for clinical applications: A consensus of the ISMRM perfusion study group and the European consortium for ASL in dementia. *Magn Reson Med*, *73*, 102–116.
- Alzheimer's Association. (2018). 2018 Alzheimer's disease facts and figures. *Alzheimers Dement*, *14*, 367–429.
- Bills, N. D., Koury, M. J., Clifford, A. J., Dessypris, E. N. (1992). Ineffective hematopoiesis in folate-deficient mice. *Blood*, *79*, 2273–2280.
- Bowyer, J. F., Tranter, K. M., Robinson, B. L., Hanig, J. P., Faubion, M. G., Sarkar, S. (2018). The time course of blood brain barrier leakage and its implications on the progression of methamphetamine-induced seizures. *Neurotoxicology*, *69*, 130–140.
- Chai, G. S., Jiang, X., Ni, Z. F., Ma, Z. W., Xie, A. J., Cheng, X. S., Wang, Q., Wang, J. Z., Liu, G. P. (2013). Betaine attenuates Alzheimer-like pathological changes and memory deficits induced by homocysteine. *J Neurochem*, *124*, 388–396.
- Chakraborty, S., Ain, R. (2017). Nitric-oxide synthase trafficking inducer is a pleiotropic regulator of endothelial cell function and signaling. *J Biol Chem*, *292*, 6600–6620.
- Chao, C. L., Lee, Y. T. (2000). Impairment of cerebrovascular reactivity by methionine-induced hyperhomocysteinemia and amelioration by quinapril treatment. *Stroke*, *31*(12), 2907–2911.
- Clarke, R., Bennett, D., Parish, S., Lewington, S., Skeaff, M., Eussen, S. J., Lewerin, C., Stott, D. J., Armitage, J., Hankey, G. J., Lonn, E., Spence, J. D., Galan, P., de Groot, L. C., Halsey, J., Dangour, A. D., Collins, R., Grodstein, F. (2014). Effects of homocysteine lowering with B vitamins on cognitive aging: Meta-analysis of 11 trials with cognitive data on 22,000 individuals. *Am J Clin Nutr*, *100*, 657–666.
- Dankner, R., Geulayov, G., Farber, N., Novikov, I., Segev, S., Sela, B. A. (2009). Cardiorespiratory fitness and plasma homocysteine levels in adult males and females. *Isr Med Assoc J*, *11*, 78–82.
- Daulatzai, M. A. (2017). Cerebral hypoperfusion and glucose hypometabolism: Key pathophysiological modulators promote neurodegeneration, cognitive impairment, and Alzheimer's disease. *J Neurosci Res*, *95*, 943–972.
- Dayal, S., Arning, E., Bottiglieri, T., Böger, R. H., Sigmund, C. D., Faraci, F., M., Lentz, S. R. (2004). Cerebral vascular dysfunction mediated by superoxide in hyperhomocysteinemic mice. *Stroke*, *35*(8), 1957–1962.
- Deacon, R. (2006). Assessing nest building in mice. *Nat Protoc*, *1*, 1117–1119.
- Durga, J., van Boxtel, M. P., Schouten, E. G., Kok, F. J., Jolles, J., Katan, M. B., Verhoef, P. (2007). Effect of 3-year folic acid supplementation on cognitive function in older adults in the FACIT trial: A randomised, double blind, controlled trial. *Lancet*, *369*, 208–216.
- Ernest, S., Hosack, A., O'Brien, W. E., Rosenblatt, D. S., Nadeau, J. H. (2005). Homocysteine levels in A/J and C57BL/6J mice: Genetic, diet, gender, and parental effects. *Physiol Genomics*, *21*, 404–410.
- Esse, R., Barroso, M., Tavares de Almeida, I., Castro, R. (2019). The contribution of homocysteine metabolism disruption to endothelial dysfunction: State-of-the-art. *Int J Mol Sci*, *20*, pii: E867.
- Ford, A. H., Almeida, O. P. (2012). Effect of homocysteine lowering treatment on cognitive function: A systematic review and meta-analysis of randomized controlled trials. *J Alzheimers Dis*, *29*, 133–149.
- Fuso, A., Nicolai, V., Cavallaro, R. A., Ricceri, L., D'Anselmi, F., Coluccia, P., Calamandrei, G., Scarpa, S. (2008). B-vitamin deprivation induces hyperhomocysteinemia and brain S-adenosylhomocysteine, depletes brain S-adenosylmethionine, and enhances PS1 and BACE expression and amyloid-beta deposition in mice. *Mol Cell Neurosci*, *37*, 731–746.
- Fuso, A., Nicolai, V., Ricceri, L., Cavallaro, R. A., Isopi, E., Mangia, F., Fiorenza, M. T., Scarpa, S. (2012). S-adenosylmethionine reduces the progress of the Alzheimer-like

- features induced by B-vitamin deficiency in mice. *Neurobiol Aging*, 33, 1482.e1–1482.e16.
- Gaskill, B. N., Karas, A. Z., Garner, J. P., Pritchett-Corning, K. R. (2013). Nest building as an indicator of health and welfare in laboratory mice. *J Vis Exp*, 82, e51012.
- Gottschall, P. E., Howell, M. D. (2015). ADAMTS expression and function in central nervous system injury and disorders. *Matrix Biol*, 44–46, 70–76.
- Hainsworth, A. H., Yeo, N. E., Weekman, E. M., Wilcock, D. M. (2016). Homocysteine, hyperhomocysteinemia and vascular contributions to cognitive impairment and dementia (VCID). *Biochim Biophys Acta*, 1862, 1008–1017.
- Howell, M. D., Torres-Collado, A. X., Iruela-Arispe, M. L., Gottschall, P. E. (2012). Selective decline of synaptic protein levels in the frontal cortex of female mice deficient in the extracellular metalloproteinase ADAMTS1. *PLoS One*, 7, e47226.
- Hudak, M. L., Koehler, R. C., Rosenberg, A. A., Traystman, R. J., Jones, M. D. Jr. (1986). Effect of hematocrit on cerebral blood flow. *Am J Physiol*, 251, H63–H70.
- Ibaraki, M., Shinohara, Y., Nakamura, K., Miura, S., Kinoshita, F., Kinoshita, T. (2010). Interindividual variations of cerebral blood flow, oxygen delivery, and metabolism in relation to hemoglobin concentration measured by positron emission tomography in humans. *J Cereb Blood Flow Metab*, 30, 1296–1305.
- Janson, J. J., Galarza, C. R., Murúa, A., Quintana, I., Przygoda, P. A., Waisman, G., Camera, L., Kordich, L., Morales, M., Mayorga, L. M., Camera, M. I. (2002). Prevalence of hyperhomocysteinemia in an elderly population. *Am J Hypertens*, 15, 394–397.
- Jiang, Y., Sun, T., Xiong, J., Cao, J., Li, G., Wang, S. (2007). Hyperhomocysteinemia-mediated DNA hypomethylation and its potential epigenetic role in rats. *Acta Biochim Biophys Sin*, 39, 657–667.
- Kilkenny, C., Browne, W. J., Cuthill, I. C., Emerson, M., Altman, D. G. (2010). Improving bioscience research reporting: The ARRIVE guidelines for reporting animal research. *PLoS Biol*, 8, e1000412.
- Kumar, M., Tyagi, N., Moshal, K. S., Sen, U., Kundu, S., Mishra, P. K., Givvimani, S., Tyagi, S. C. (2008). Homocysteine decreases blood flow to the brain due to vascular resistance in carotid artery. *Neurochem Int*, 53(6–8), 214–209.
- Kuo, H. K., Yen, C. J.s., & Bean, J. F. (2005). Levels of homocysteine are inversely associated with cardiovascular fitness in women, but not in men: Data from the National Health and Nutrition Examination Survey 1999–2002. *J Intern Med*, 258, 328–335.
- Lanier, J. B., Park, J. J., & Callahan, R. C. (2018). Anemia in older adults. *Am Fam Phys*, 98, 437–442.
- Lee, H., Kim, H. J., Kim, J.-M., Chang, N. (2004). Effects of dietary folic acid supplementation on cerebrovascular endothelial dysfunction in rats with induced hyperhomocysteinemia. *Brain Res*, 996(2), 139–147.
- Ma, D., Wang, A. C., Parikh, I., Green, S. J., Hoffman, J. D., Chlipala, G., Murphy, M. P., Sokola, B. S., Bauer, B., Hartz, A. M. S., Lin, A. L. (2018). Ketogenic diet enhances neurovascular function with altered gut microbiome in young healthy mice. *Sci Rep*, 8, 6670.
- Margalit, I., Cohen, E., Goldberg, E., Krause, I. (2018). Vitamin B12 deficiency and the role of gender: A cross-sectional study of a large cohort. *Ann Nutr Metab*, 72, 265–271.
- Michel, T., Vanhoutte, P. M. (2010). Cellular signaling and NO production. *Pflügers Arch*, 459, 807–816.
- Morris, M. S., Jacques, P. F., Selhub, J., Rosenberg, I. H. (2000). Total homocysteine and estrogen status indicators in the Third National Health and Nutrition Examination Survey. *Am J Epidemiol*, 152, 140–148.
- Novaković, R., Geelen, A., Ristić-Medić, D., Nikolić, M., Souverein, O. W., McNulty, H., Duffy, M., Hoey, L., Dullemeijer, C., Renkema, J. M. S., Gurinović, M., Glibetić, M., de Groot, L. C. P. G. M., Van't Veer, P. (2018). Systematic review of observational studies with dose-response meta-analysis between folate intake and status biomarkers in adults and the elderly. *Ann Nutr Metab*, 73, 30–43.
- Oller, J., Méndez-Barbero, N., Ruiz, E. J., Villahoz, S., Renard, M., Canelas, L. I., Vriones, A. M., Alberca, R., Lozano-Vidal, N., Hurlé, M. A., Milewicz, D., Evangelista, A., Salaices, M., Nistal, J. F., Jiménez-Borreguero, L. J., De Backer, J., Campanero, M. R., Redondo, J. M. (2017). Nitric oxide mediates aortic disease in mice deficient in the metalloprotease Adamts1 and in a mouse model of Marfan syndrome. *Nat Med*, 23, 200–212.
- Patching, S. G. (2017). Glucose transporters at the blood-brain barrier: Function, regulation and gateways for drug delivery. *Mol Neurobiol*, 54, 1046–1077.
- Price, B. R., Wilcock, D. M., Weekman, E. M. (2018). Hyperhomocysteinemia as a risk factor for vascular contributions to cognitive impairment and dementia. *Front Aging Neurosci*, 10, 350.
- Rodríguez-Baena, F. J., Redondo-García, S., Peris-Torres, C., Martino-Echarri, E., Fernández-Rodríguez, R., Plaza-Calonge, M. D. C., Andersson, P., Rodríguez-Manzanque, J. C. (2018). ADAMTS1 protease is required for a balanced immune cell repertoire and tumour inflammatory response. *Sci Rep*, 8, 13103.
- Ruiz, J. R., Sola, R., Gonzalez-Gross, M., Ortega, F. B., Vicente-Rodriguez, G., Garcia-Fuentes, M., Gutierrez, A., Sjöström, M., Pietrzik, K., Castillo, M. J. (2007). Cardiovascular fitness is negatively associated with homocysteine levels in female adolescents. *Arch Pediatr Adolesc Med*, 161, 166–171.
- Salles-Montaudon, N., Parrot, F., Balas, D., Bouzigon, E., Rainfray, M., Emeriau, J. P. (2003). Prevalence and mechanisms of hyperhomocysteinemia in elderly hospitalized patients. *J Nutr Health Aging*, 7, 111–116.
- Sassi, S., Cosmi, B., Palareti, G., Legnani, C., Grossi, G., Musolesi, S., Coccheri, S. (2002). Influence of age, sex and vitamin status on fasting and post-methionine load plasma homocysteine levels. *Haematologica*, 87, 957–964.
- Selhub, J. (1999). Homocysteine metabolism. *Annu Rev Nutr*, 19, 217–246.
- Smith, A. D., Smith, S. M., de Jager, C. A., Whitbread, P., Johnston, C., Agacinski, G., Oulhaj, A., Bradley, K. M., Jacoby, R., Refsum, H. (2010). Homocysteine-lowering by B vitamins slows the rate of accelerated brain atrophy in

- mild cognitive impairment: A randomized controlled trial. *PLoS One*, 8, e12244.
- Smith, A. D., Refsum, H., Bottiglieri, T., Fenech, M., Hooshmand, B., McCaddon, A., Miller, J. W., Rosenberg, I. H., Obeid, R. (2018). Homocysteine and dementia: An international consensus statement. *J Alzheimers Dis*, 62, 561–570.
- Sudduth, T. L., Powell, D. K., Smith, C. D., Greenstein, A., Wilcock, D. M. (2013). Induction of hyperhomocysteinemia models vascular dementia by induction of cerebral microhemorrhages and neuroinflammation. *J Cereb Blood Flow Metab*, 33, 708–715.
- Sudduth, T. L., Weekman, E. M., Price, B. R., Gooch, J. L., Woolums, A., Norris, C. M., Wilcock, D. M. (2017). Time-course of glial changes in the hyperhomocysteinemia model of vascular cognitive impairment and dementia (VCID). *Neuroscience*, 341, 42–51.
- Thai, S. N., Iruela-Arispe, M. L. (2002). Expression of ADAMTS1 during murine development. *Mech Dev*, 115, 181–185.
- Troen, A. M., Shea-Budgell, M., Shukitt-Hale, B., Smith, D. E., Selhub, J., Rosenberg, I. H. (2008). B-vitamin deficiency causes hyperhomocysteinemia and vascular cognitive impairment in mice. *Proc Natl Acad Sci U S A*, 105, 12474–12479.
- Van Dam, F., Van Gool, W. A. (2009). Hyperhomocysteinemia and Alzheimer's disease: A systematic review. *Arch Gerontol Geriatr*, 48, 425–430.
- Webster, S. J., Eldik, L. J., Watterson, D. M., Bachstetter, A. D. (2015). Closed head injury in an age-related Alzheimer mouse model leads to an altered neuroinflammatory response and persistent cognitive impairment. *J Neurosci*, 35, 6554–6569.
- Wu, X., Sun, J., & Li, L. (2013). Chronic cerebrovascular hypoperfusion affects global DNA methylation and histone acetylation in rat brain. *Neurosci Bull*, 29, 685–692.
- Yan, T. T., Li, Q., Zhang, X. H., Wu, W. K., Sun, J., Li, L., Zhang, Q., Tan, H. M. (2010). Homocysteine impaired endothelial function through compromised vascular endothelial growth factor/Akt/endothelial nitric oxide synthase signalling. *Clin Exp Pharmacol Physiol*, 37, 1071–1077.
- Zhang, F., Slungaard, A., Vercellotti, G. M., Iadecola, C. (1998). Superoxide-dependent cerebrovascular effects of homocysteine. *Am J Physiol Regul Integr Comp Physiol*, 274(6), R1704–R1711.
- Zimmermann, K., Opitz, N., Dedio, J., Renne, C., Muller-Esterl, W., Oess, S. (2002). NOSTRIN: A protein modulating nitric oxide release and subcellular distribution of endothelial nitric oxide synthase. *Proc Natl Acad Sci U S A*, 99, 17167–17172.